Microporous and Mesoporous Materials 120 (2009) 460-466

Controlled synthesis of high performance carbon/zeolite T composite membrane materials for gas separation

Q. Liu[a], T. Wang,[a]* H. Guo[b], C. Liang[a], S. Liu[a], Z. Zhang[b], Y. Cao[c], D. S. Su[d], J. Qiu[a]

[a]State Key Laboratory of Fine Chemicals, Carbon Research Laboratory, Department of Materials Science and Chemical Engineering, School of Chemical Engineering, Dalian University of Technology, Dalian 116012, PR China

[b]Department of Catalysis Chemistry and Engineering, School of Chemical Engineering, Dalian University of Technology, Dalian 116012, PR China

[c]Dalian Institute of Chemical Physics, Chinese Academy of Sciences, Dalian 116023, PR China

[d]Department of Inorganic Chemistry, Fritz Haber Institute of the Max Planck Society, Faradayweg 4–6, 14195 Berlin, Germany

* Corresponding author: Tel./fax: +86 411 88993968

Received 27 June 2008; revised 10 December 2008; accepted 19 December 2008. Available online 13 January 2009.

Abstract

A simple and versatile approach has been developed to synthesize different carbon/zeolite T functional membrane materials. The precursors of the membrane are composed of polyimide matrix and dispersed zeolite T particles. Membranes prepared by pyrolysis at 973 K showed excellent gas (H_2, CO_2, O_2, N_2, CH_4) permeability and selectivity and the gas selectivity (O_2/N_2, CO_2/CH_4) of the functional membranes for both single gas and mixed-gas can be controlled in a wide range by changing the zeolite T particle size and morphology without altering the final pyrolysis temperature and zeolite loadings. The maximum achieved selectivity for O_2 over N_2 (21/79 mol. %) of the functional membranes with the least zeolite T particle (0.5 μm) was 15 with an O_2 permeability of 347 Barrers (1 Barrer=7.5×10^{-18} m^2 s^{-1} Pa^{-1}) and the CO_2 over CH_4 (50/50 mol. %) selectivity reached a value of 179 with a CO_2 permeability of 1532 Barrers. It is believed that the ordered microchannels in the zeolite and the bypasses around zeolite in the functional membranes increase the gas permeability. And the gas selectivity of the membranes was tuned by the interfacial gaps between zeolite and carbon phase via changing the zeolite particle size. This technique will provide a simple and convenient route to efficiently improve the trade-off relationship between the permeability and the selectivity, and will enable the construction of carbon-based functional materials with novel functionalities in membrane science.

Keywords: Carbon; Zeolite; Polyimide; Composite membrane; Gas separation

1. Introduction

Compared to conventional separation techniques, membrane-based gas separation become more attractive for their low energy consumption and environmental friendly characterization.[1] In particular, membranes made from polymeric materials have been widely used for gas separation such as O_2 separation from air, the separation and recovery of the CO_2 and small molecular hydrocarbon gases from natural gas and exhaust gases produced by coal-fired power plants and chemical or petroleum factories owing to their relatively low cost and ease of being processed into hollow fibers.[2] However, the swelling-induced plasticization of the polymeric membranes by CO_2 and hydrocarbons under the high pressure caused their performance decline, which negatively impacts process economics and reliability.[2] A more promising choice is carbon membranes, a novel inorganic membrane material for gas separation. The significant advantage of the carbon membranes is that they can separate small gas molecules

under harsh conditions such as elevated temperature and pressure. Also, the carbon membranes have a molecular sieving capability rendered by their ultramicropore structure with dimensions near the size of the permeating gas molecules, which help them to achieve a desirable and practicable selectivity.[3] Up to date, carbon membranes are typically prepared from inert or vacuum pyrolysis of various polymeric materials such as poly (furfuryl alcohol),[4] phenolic resins,[5] poly (phthalazinone ether sulfone ketone),[6] coal tar pitch,[7] and polyimide (PI).[8-12] However, the challenge of this membrane materials is that the permeation flux is considerably reduced with increased gas selectivity due to the disordered pore structure and diffusion resistance in membranes, The carbon membrane with high selectivity has a low gas permeability, which can not satisfy the practical application requirement.

A novel development for improving the gas permeability and selectivity of carbon membranes is to functionalize the membrane by incorporating metals or inorganic particles into the membrane precursors. Barsema et al.[13] dispersed the nano-sized Ag particles into carbon matrix to enhance the O_2/N_2 selectivity due to the stronger adsorption of Ag to O_2. Kim et al.[14] prepared carbon membranes containing alkali metal ions (Li^+, Na^+, and K^+) and found the gas permeability of carbon membranes increased with increasing the ionic radius of substituted metal ions. Yoda et al.[15] incorporated Pt and Pd nano-particles into carbon matrix by the supercritical impregnation method, and the hydrogen selectivity of the resultant membranes was 17 times higher than that of non-doped membranes. Zhang et al.[16], Yoshimune et al.[17] and Hägg et al.[18] also reported their research works on the metal-doped carbon membranes with different metals and all showed some improvement on gas permeability and selectivity of resultant carbon membranes. Besides the metals, inorganic particles were also used as the functional groups to modify the gas separation performance of carbon membranes. Park et al.[19] showed that the incorporation of silica dioxide particles into carbon matrix by sol-gel method or mixing polymeric precursors with siloxane significantly improved the gas separation performances of carbon/silica membranes owing to the gas molecular fast diffusion in the amorphous microporous silica domains. Tin et al.[20] filled the zeolite KY into polymeric precursors to prepare a zeolite-filled carbon membrane, and the CO_2/CH_4 selectivity of zeolite-filled carbon membranes was twice of pure carbon membrane. Jiang et al.[21] fabricated a dual-layer carbon-zeolite beta hollow fiber carbon membrane via pyrolyzing the polysulfone-beta zeolite precursor and found the carbon-zeolite beta carbon membrane showed a higher gas selectivity than that of no zeolite.

Recently, our group have made the research works on improving the gas separation performance of the carbon membranes by functionalizing the membrane with zeolite. The gas permeability of the ZSM-5 functionalized carbon membranes was significantly improved by nano-ZSM-5 without losing the gas selectivity because the ordered pore channel in zeolite could reduce the gas permeation resistance through the membrane. And their gas separation performance could be tuned via changing the zeolite loadings and the final pyrolysis temperatures.[22]. In this paper, a novel zeolite material, the zeolite T, was chosen to prepare the zeolite-functionalized carbon membranes. Zeolite T is an intergrowth-type zeolite of erionite and offretite, of which the effective pore size is 0.36 nm × 0.51 nm.[23] The microchannels are beneficial to the small molecules to permeate through zeolite T such as O_2 and CO_2 with a kinetic diameter of 0.346 nm and 0.33 nm and block the large molecules such as N_2 and CH_4 with of 0.364 nm and 0.38 nm to go through the zeolite. In the zeolite T-functionalized carbon membrane, the micro-channels in zeolite and interface gaps formed between zeolite and carbon matrix will act as the permeation routeways for small gas molecules and improve gas permeability of the membrane. Moreover, the gas permselectivity of the functional membrane can be tuned and controlled in a wide range by variating the particle size and morphology of zeolite T without altering the final pyrolysis temperature and zeolite loadings.

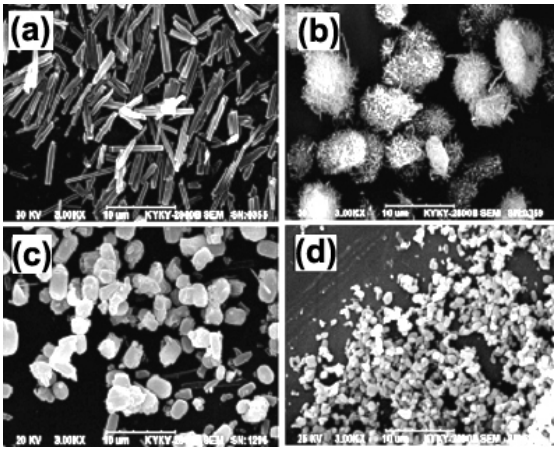

Fig. 1: SEM images zeolite T: (a) ZT-8; (b) ZT-6; (c) ZT-3; (d) ZT-0.5.

2. Results and Discussion

2.1 Precursors of the carbon/zeolite T functional membranes

The precursors of the functional membrane were composed of zeolite T particle and polyamic acid (PAA) derived from pyromellitic dianhydride and 4, 4-oxydianiline. Four kinds of zeolite T with different morphology and size (ZT-8: 8 μm, ZT-6: 6 μm, ZT-3: 3 μm, ZT-0.5: 0.5 μm) were prepared by the hydrothermal synthesis method. Figure 1 shows the morphology of the as-synthesized zeolite T. The zeolite ZT-8 is bar-shape crystal with 8 μm long and 1 μm wide. The zeolite ZT-6 is ball-shape with a diameter of about 6 μm, which is assembled

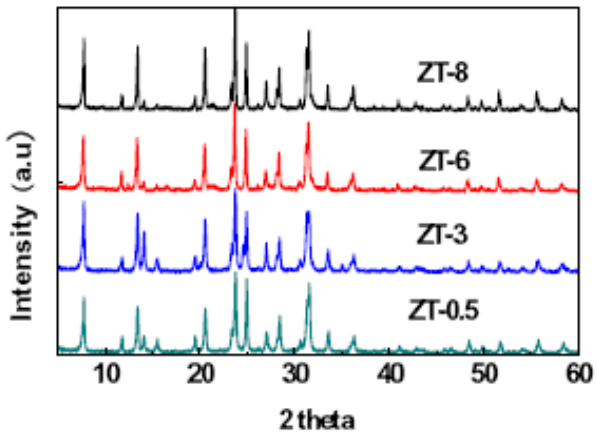

Fig. 2: XRD patterns of pure zeolite T: ZT-8, ZT-6, ZT-3, and ZT-0.5.

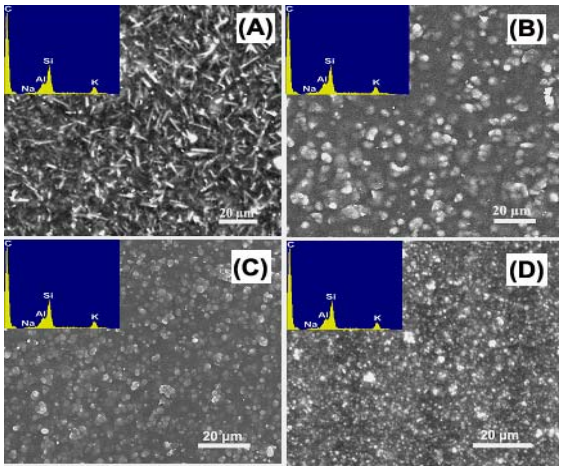

Fig. 3: The top surface SEM images of the carbon/zeolite T functional membranes prepared under 973 K with their EDX spectra: (A): ZTC-8; (B): ZTC-6; (C): ZTC-3; (D) ZTC-0.5.

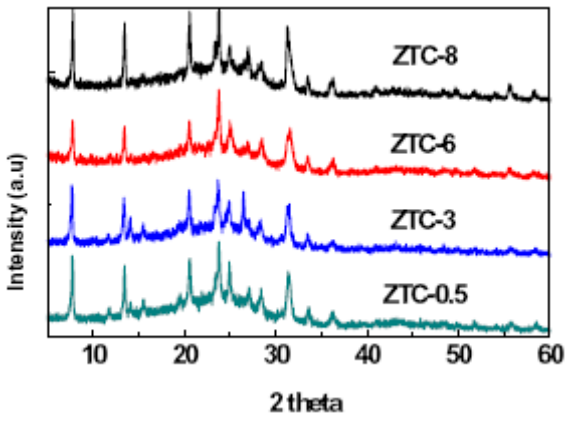

Fig. 4: The XRD patterns of the carbon/zeolite T functional carbon membranes (ZTC-8, ZTC-6, ZTC-3, ZTC-0.5) prepared under 973K

from small zeolite T crystals. The zeolite ZT-3 and ZT-0.5 are ellipse crystals with the diameter around 3 μm and 0.5 μm respectively. Figure 2 shows their typical X-ray diffraction patterns, which confirmed that the zeolites were synthesized successfully.

The as-obtained zeolite T crystals were first dispersed in PAA solution respectively to form homogeneous PAA/zeolite T mixed matrix solutions under stirring and ultrasonic process, and the content of zeolite T in each solution was controlled to be 10 wt. %. Following a prepolymerization step, the solution was cast on a glass plate and dried at 313K. The resulting PAA/zeolite T precursors were used to prepare the self-supporting carbon/zeolite T functional membranes (denoted as: ZTC-8, ZTC-6, ZTC-3, ZTC-0.5) by pyrolysis at 973 K under flowing argon stream.

2.2 SEM images of the carbon/zeolite T functional membranes

The top surface morphology of the carbon/zeolite T functional membranes is shown in Figure 3. The white spots indicate the zeolite T crystals, and the black spots indicate the carbon domains. In the case of ZTC-8 (Figure 3 A), the zeolite T crystals are disordered dispersed in the carbon matrix, which could be caused by the bar-shape effect. For ZTC-6, ZTC-3, and ZTC-0.5 (Figure 3 B, 3 C, 3 D), the ball-shape and ellipse-shape crystals are well dispersed in carbon matrix with their original diameter. No voids and defects between the zeolite crystal and the carbon phase are observed in all samples, suggesting good zeolite/carbon contact. The inserted energy-dispersive X-ray spectrometry (EDX) analysis confirmed that the functional membrane is composed of carbon (C) and zeolite T (Na, Al, Si, K). Since the content of zeolite T in all functional membrane precursors are the same (10 wt. %), the element contents in all the samples are close to each other.

2.3 XRD patterns of the carbon/zeolite T functional membranes

Figure 4. shows the XRD patterns of the carbon/zeolite T functional membranes. Generally, only a broad weak (002) peak can be seen in the traditional pure carbon membranes, which were attributed to the turbostratic carbon structure with randomly oriented graphitic carbon layers.[24] In the case of the functional carbon membranes, however, peaks with zeolite T and carbon character can be observed. As shown in Figure 4, the typical zeolite T X- ray diffraction patterns in the ZTC-8, ZTC-6 ZTC-3 and ZTC-0.5 indicate that the structure of zeolite T is not destroyed during the heat treatment. The well-kept zeolite structure is believed to be one of the most important factors in affecting the gas separation performance of the functional membranes. The microchannels in zeolite could help increase the porosity of the membranes and decrease the

gas molecular diffusion resistance. The XRD study also reveals that no significant changes are observed in the crystal size of the zeolite T before and after being incorporated into the membranes, indicating good zeolite dispersion.

2.4 Gas separation performance of the carbon/zeolite T functional membranes

Single gas permeation (H_2, CO_2, O_2, N_2, and CH_4) and mixed-gas (21/79 mol. % O_2/N_2, 50/50 mol. % CO_2/CH_4) permeation tests were carried out through the carbon/zeolite T membranes. The samples were measured by the variable volume-constant pressure method followed by the gas- chromatogram analysis of the permeation at a feed pressure of 100 kPa at 298K.

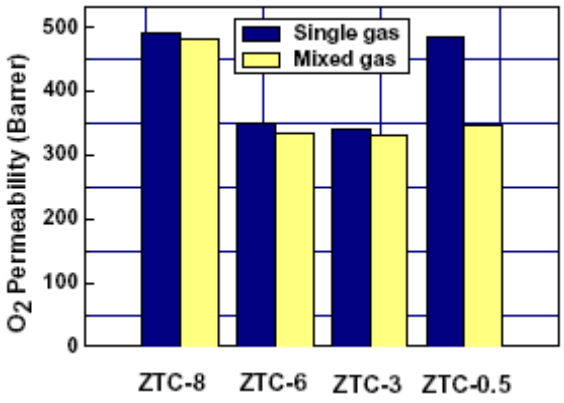

Fig. 5: The O_2 permeability for singe gas and mixed-gas (21/79 mol. %) permeation in ZTC-8, ZTC-6, ZTC-3, and ZTC-0.5 membranes at 100 kPa and a temperature of 298 K.

2.4.1 O_2/N_2 separation

As shown in Figure 5, the permeability of O_2 in the carbon/zeolite T functional membranes for both single gas and mixed-gas were around 330-490 Barrers which is much higher than that in polymeric membranes and pure carbon membranes.[22] The dramatic increase of gas permeability in the functional membranes should be contributed the zeolite T crystals embedded in carbon matrix. It is well known that zeolite T is a crystalline microporous material with an intricate channel system and uniform pores (0.36 nm × 0.51 nm). The continuous microchannels presented in the composites allow the small gas molecules to diffuse quickly through the zeolite. Furthermore, the zeolite T crystals may help to create interfacial gaps between zeolite and carbon matrix due to the effect of micro-phase separation, which may increase the permeability of gas molecules through the membranes.

Compared to single gas, the O_2 permeability in mixed-gas is somewhat lower in the functional membranes. This phenomenon should be contributed to the "competitive permeance" effect between the gas pairs through the membranes. That is, the gas molecule in mixed-gas would obstruct each other when they pass through the membrane simultaneously, which result a lower permeability and higher selectivity (Figure 6) compared to the single-compone nt gas permeation.

It is interesting that the permeability and selectivity of the functional carbon membranes is dramatically affected by the zeolite size and morphology. As shown in Figure 5 and Figure 6, the O_2/N_2 selectivity obviously increases with the reduction of zeolite size (O_2/N_2 selectivity: ZTC-8<ZTC-6<ZTC-3<ZTC-0.5). The sample ZTC-8, with bar-shape and a zeolite size of 8 μm, shows the highest O_2 permeability and lowest O_2/N_2 selectivity, and the sample ZTC-0.5, with a zeolite size of 0.5 μm, shows a higher O_2 permeability and the highest O_2/N_2 selectivity (13 and 15 for single gas and mixed-gas respectively). This

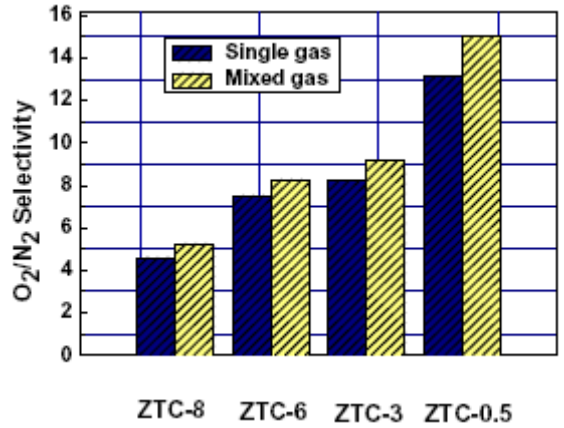

Fig.6: The O_2 permeability for singe gas and mixed-gas (21/79 mol. %) permeation in ZTC-8, ZTC-6, ZTC-3, and ZTC-0.5 membranes at 100 kPa and a temperature of 298 K.

may be explained by the effects of zeolite size and morphology. That is, the different zeolite size and morphology might make the as-prepared functional membranes form different micropore structures. As shown in the SEM images (Figure 3 (A)), the bar-shape zeolite T with the largest size was randomly dispersed in the carbon matrix, which would create much more wide interfacial gaps between the carbon matrix and zeolite, and lead to a higher gas permeability for both O_2 and N_2, which lower the O_2/N_2 selectivity. On the other hand, for the small zeolite, the interfacial gaps formed between the carbon matrix and zeolite should be smaller owing to their small single crystal volume. Thus, the larger gas molecular such as N_2 would difficult pass through the membrane, and the selectivity of the functional membrane with small zeolite is much higher than that with large zeolite. Besides, due to the same zeolite loading used in all the samples (10 wt. %), the crystal particle number of the zeolite with large size should be fewer than that of the zeolite with small size. The number of total interfacial gaps

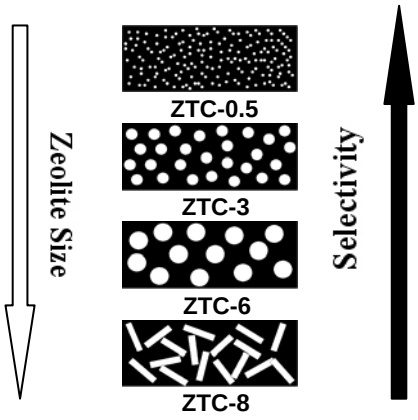

Fig. 7: The ideal model of ZTC-8, ZTC-6, ZTC-3, and ZTC-0.5, respectively.

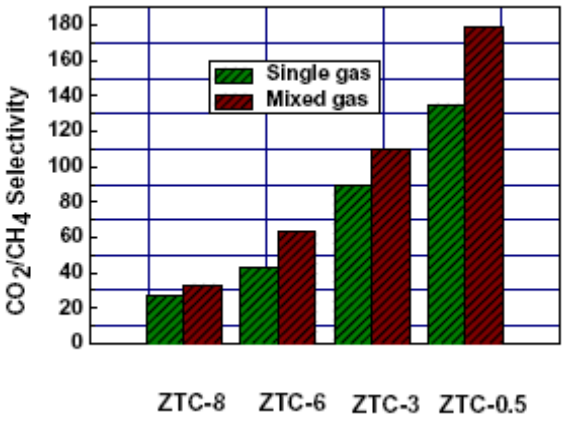

Fig. 9: The CO_2/CH_4 selectivity for singe gas and mixed-gas (50/50 mol. %) permeation in ZTC-8, ZTC-6, ZTC-3, and ZTC-0.5 membranes at 100 kPa and a temperature of 298 K.

formed in the functional membranes with smaller zeolite should be much more than those in the functional mem branes with larger zeolite; therefore, the functional membrane with smaller zeolite exhibits higher gas permeability. Figure 7 shows the ideal model of ZTC-8, ZTC-6, ZTC-3, and ZTC-0.5 respectively. The interesting results obtained above suggest that the gas permeability and selectivity of the functional membrane can be tuned and controlled by varying the zeolite size and morphology without changing the zeolite loadings and pyrolysis condition.

2.4.1 CO_2/CH_4 separation

For the CO_2/CH_4 gas pairs, as shown in Figure 8 and Figure 9, the change of gas permeability and selectivity for the functional membranes with the zeolite size and morphology exhibit the same way as for the O_2/N_2 separation. The permeability of CO_2 for mixed-gas in all samples is about 200 Barres lower than that in single gas owing to the "competitive permeance" effect. The CO_2/CH_4 selectivity for both single and mixed-gas in the functional membranes also increases as the zeolite T size decreases, and the membrane with the least zeolite T ZTC-0.5 reached the maximum value of 135 and 179 respectively (Figure 9). This is because the micropore size of the functional membrane becomes narrower with the reduction of zeolite size, which made the CH_4 difficult to permeate the membrane. Further more, the CO_2 has higher adsorption capability in zeolite T microchannels. Thus, CO_2 is preferred to be adsorbed in zeolite and blocks the CH_4 molecules through the zeolite T channels in the functional membranes for the CO_2/CH_4 mixed gas.[25] The synergetic effects of competitive adsorption and "competitive permeance" make the membrane show higher selectivity for gas mixtures.

2.5 The pore structure and gas separation mechanism of the carbon/zeolite T functional membranes

Mass transfer of gas through a porous membrane can involve several processes, depending on the nature of the pore structure. To confirm the effect of the zeolite particle size on the pore structure and gas permeation of the functional membranes, nitrogen adsorption experiment was performed. As shown in Figure 10, the nitrogen adsorption isotherms of all the functional membrane samples are I type according to the IUPAC classification, which suggests that they are microporous materials. The median pore size of the samples estimated using the H-K method are in the order of ZTC-8 (0.517 nm) > ZTC-6 (0.479 nm) > ZTC-3 (0.465 nm) > ZTC-0.5 (0.447 nm), and the micropore surface area of the samples estimated using the Dubinin–Astakhov (D-A) equation are in the order of ZTC-8 (307 cm^2g^{-1}) <ZTC-6 (475 cm^2g^{-1}) < ZTC-3 (535 cm^2g^{-1}) < ZTC-0.5 (642 cm^2g^{-1}), which is exactly in accordance with the order of the gas selectivity of the functional membranes. These results clearly indicate that the pore structure of the functional membranes were influenced by the zeolite T particle size, and the structural properties of the functional membranes agree with the gas permeation results described above. This also further confirms the explanation about the relationship of the gas separation performance of the functional membranes with the size and morphology of the zeolite T.

The gas permeabilities of the selected gases in all the carobn/zeolite T functional membranes were in the order: H_2 (0.289 nm) > CO_2 (0.33 nm) > O_2 (0.346) > N_2 (0.364 nm) > CH_4 (0.38 nm), which is in agreement with the order of their kinetic gas diameters (Figure 11). Usually, the transport mechanism of a molecular sieving material is based on this mechanism. According to this mechanism, the separation is caused by the passage of smaller molecules through the pores while the larger molecules are obstructed. It is indicated that the gas permeation

in the carbon/zeolite T functional membranes obeys the molecular sieving mechanism. Another character of the functional membrane is that the CO_2 can be quickly adsorbed and diffused in zeolite T due to the interaction of the electric field in zeolite T and quadrupole moment of CO_2. The strong affinity of CO_2 molecules to zeolite T resulted in high adsorption coverage of CO_2 in zeolite pores and a high permeability. In this view, the mechanism of the CO_2 permeation in the carbon/zeolite T functional membranes should be the synergistic effects of molecular sieving and surface diffusion/selective adsorption.

3. Conclusions

In summary, carbon/zeolite T functional membranes were successfully synthesized by incorporating zeolite T crystals into the carbon matrix. Compared to the conventional pure carbon membranes derived from polymers, the functional membranes exhibit an excellent gas separation performance. The membrane contained the least zeolite (0.5 μm) exhibited the highest O_2/N_2 selectivity of 15 and CO_2/CH_4 selectivity of 179 for mixed-gas permeation test without losing the gas permeability. The gas permeability and selectivity of the functional membranes is dramatically affected by the zeolite size and morphology. This suggests that the pore structure and gas separation performance of the functional membranes can be tuned and controlled by the size and morphology of the zeolite T. The method presented here could extend to prepare other functional membranes containing different zeolite, such as faujasite (FAU), zeolite L (LTL), ZSM-5 (MFI), and zeolite beta (BEA) etc. Such a high performance functional membranes could be used to enrich the oxygen or nitrogen and separate, recycle the CO_2 from the exhaust gases produced by coal-fired power plants, chemical factories, and natural gas purification.

4. Experimental

Membrane Preparation: Zeolite T crystals were synthesized by hydrothermal synthesis from clear gel solutions. The dry zeolite T (0.63 g) was first dispersed in N, N-Dimethylacetamide (DMAc) under stirring and ultrasonic treatment for 2h. Then, the suspension was mixed with poly (amic acid) (PAA) solution (20 g, 24 wt%) derived from pyromellitic dianhydride (PMDA) and 4, 4'-oxydianiline (ODA) Following a prepolymerization step at 298 K for 10 h, a homogeneous solution was cast on a glass plate and dried for 12h at 313 K to obtain the PAA/zeolite T functional membranes. The composition of the zelite T in PAA/zeolite matrix is 10 wt. %. Then, the PAA/zeolite T functional membranes were pyrolyzed between graphite blocks 973 K for 2h in flowing argon of 100 ml min^{-1} with a heating rate of 2 K min^{-1}.

Characterization Methods: Wide-angle X-ray diffraction was performed to qualitatively measure the structure of the zeolite functional membranes on a diffractometer equipped with graphite-monochromatized Cu Ka radiation in the 2θ angle range from 5° to 60°. The SEM images were observed by a JEOL-5600LV scanning electron microscopy (JEOL, Inc., Kyoto, Japan). The porous structure of the membranes was characterized by nitrogen sorption (Micromeritics ASAP 2020 pore sizer) after degassing at 300 °C.

Gas Permeation Measurements: Single-component gas permeation (O_2, N_2, CO_2, CH_4, purity >99.99%) was carried out through the as-obtained carbon/zeolite T membranes by means of the variable volume-constant pressure method. The permeability coefficient for a permeated gas is determined by multiplying the permeance by the membrane thickness and can be obtained by

$$P = \frac{R}{A \cdot \Delta P / l} \tag{1}$$

where P is the permeability represented in Barrer (1 Barrer = 10^{-10} cm^3 (STP)cm/cm^2 s cmHg); R is the flux of gas permeating the membrane; A and l are the effective membrane area and membrane thickness, respectively; ΔP is the pressure difference between the feed side and the permeate side. The ideal separation factor (gas selectivity) for components A and B is defined as the ratio of permeability of each component as

$$S_{A/B} = \frac{P_A}{P_B} \tag{2}$$

Mixed-gas (21/79 mol. % O_2/N_2, 50/50 mol. % CO_2/CH_4) were measured by the variable volume-constant pressure method followed by the gas-chromatogram analysis of permeate gas at a feed pressure of 100 kPa at 25°C. The feed gas is flowed across one side of a membrane at a rate of 4 ml/min and the permeate sweep gas (Ar) flow is controlled by a mass flow controller at a rate of 2 ml/min. The total permeate flow during testing is calculated by formula (1). The permeate gas flows are directed by a series of automated valves through a gas chromatograph (GC) for analysis. The real selectivities of mixed-gas was calculated as

$$S_{A/B} = \frac{y_A / y_B}{x_A / x_B} \tag{3}$$

Where y and x are, respectively, the molar fractions at the feed side and the permeation side. GC analyses were made using a GC 7890 (Techcomp LTD.) equipped with a thermal conductivity detector (TCD). Two different columns were required for this work. For O_2 and N_2 analysis, a 5A molecular sieve 3m×3mm ID column was employed. For CO_2 and CH_4, a carbon molecular sieve 2m×4mm ID column was used. The effective area of the membranes was 6 cm^2. For each membrane, measurements were conducted

with more than three samples prepared at same time, and the final results reported are the averaged ones.

References

[1] a) H. Lin, E. V. Wagner, B. D. Freeman, L. G. Toy, R. P. Gupta, *Science* **2006**, *311*, 639; b) H. Lin, E. V. Wagner, R. Raharjo, B. D. Freeman, I. Roman, *Adv. Mater.* **2006**, *18*, 39; c) Z. Lai, G. Bonilla, I. Diaz, J. G. Nery, K. Suiaoti, M. A. Amat, E. Kokkoli, O. Terasaki, R. W. Thompson, M. Tsapatsis, D. G. Vlachos, *Science* **2003**, *300*, 456.

[2] a) J. H. Kim, W. J. Koros, D.R. Paul, *J. Membr. Sci.* **2006,** *282,* 21; b) S. Kanehashi, T. Nakagawa, K. Nagai, X. Duthie, S. Kentish, G. Stevens, *J. Membr. Sci.* **2007**, *298*, 147.

[3] a) A. F. Ismail, L. I. B. David, *J. Memr. Sci.* **2001**, *193,* 1; b) S. M. Saufi, A. F. Ismail. *Carbon.* **2004**, *42,* 241.

[4] a) M. B. Shiflett, H. C. Foley, Science **1999**, *285*, 1902; b) M. B. Shiflett, J. F. Pedrick, S. R. Mclean, S. Subramoney, H. C. Foley, *Adv. Mater*. **2000**, *12*, 21; c) R. Rajagopalan, A. Merritt, A. Tseytlin, H. C. Foley, *Carbon*, **2006,** *44*, 2051; d) A. Merritt, R. Rajagopalan, H. C. Foley, *Carbon*. **2007,** *45*, 1267.

[5] a) X. Zhang, H. Hu, Y. Zhu, S. Zhu, *J. Membr. Sci.* **2007,** *289*, 86*;* b) W. Zhou, M. Yoshino, H. Kita, K Okamoto, *J. Membr. Sci.* **2003,** *217,* 55. c) T. A. Centeno, J. L. Vilas, A. B. Fuertes, *J. Membr. Sci.* **2004,** *228,* 45.

[6] B. Zhang, T. H. Wang, S. H. Zhang, J. S. Qiu, X. G. Jian, *Carbon*, **2006,** *44*, 2764.

[7] C. H. Liang, G.Y. Sha, S. C. Guo, *Carbon*. **1999**, *37*, 1391.

[8] a) L. Shao, T. S Chung , K. P. Pramoda, *Microporous Mesoporous.Mater*. **2005**, *84*, 59; b) P. S. Tin, T. S. Chung, A. J. Hill, *Ind. Eng. Chem. Res.* **2004**, *43,* 6476.

[9] K. M. Steel, W. J. Koros, *Carbon*. **2005**, *43*, 1843.

[10] H. Suda, K. Haraya, *J. Phys. Chem. B* **1997**, *101*, 3988.

[11] J. Hayashi, H. Mizuta, Y. Yamamoto, K. Kusakabe, S. Morooka, *J. Membr. Sci*. **1997**, *124,* 243.

[12] A. B. Fuertes, D. M. Nevskaia, T. A. Centeno, *Microporous Mesoporous Mater*. **1999**, *33*, 115.

[13] a) J. N. Barsema, J. Balster, V. Jordan, N. F. A. Van der Vegt, M. Wessling, *J. Membr. Sci.* **2003**, *219*, 47. b) J. N. Barsema, N. F. A. Van der Vegt, G. H. Koops, M. Wessling, *Adv. Funct. Mater.***2005,** *15,* 69.

[14] Y. K. Kim, H. B. Park, Y. M. Lee, J. *Membr. Sci.* **2003**, *226*,145.

[15] S. Yoda, A. Hasegawa, H. Suda, Y. Uchimaru, K. Haraya, T. Tsuji, K. Otake, *Chem. Mater*. **2004**, *16,* 2363.

[16] L. X. Zhang, X. H. Chen, C. F. Zeng, N. P. Xu, *J. Membr. Sci.* **2006,** *281,* 429.

[17] M. Yoshimune, I. Fujiwara, H. Suda, K. Haraya, *Desalination*. **2006**, *193,* 66.

[18] J. A. Lie, M. –B. Hägg, *J. Membr. Sci.* **2006,** *284,* 79.

[19] a) H. B. Park, Y. M. Lee, *Adv. Mater.* **2005,** *17,* 477. b) H. B. Park, I. Y. Suh, Y. M. Lee, *Chem. Mater*. **2002**, *14*, 3034. c) H. B. Park, Y. M. Lee, *J. Membr. Sci.* **2003**, *213*, 263. d) H. B. Park, C. H. Jung, Y. K. Kim, S. Y. Lee, S. Y. Nam, Y. M. Lee, *J. Membr. Sci.***2004**, *235,* 87.

[20] P. S. Tin, T. S. Chung, L. Y. Jiang, S. Kulprathipanja, *Carbon*, **2005,** *43*, 2013.

[21] L. Y. Jiang, T. S. Chung, R. Rajagopalan, *Carbon*, **2007,** *45*, 166.

[22] a) Q. L. Liu, T. H. Wang, J. S. Qiu, Y. M. Cao, *Chem. Commun.* **2006**, 1230. b) Q. L. Liu, T. H. Wang, C. H. Liang, B. Zhang, S. L. Liu, Y. M. Cao, J. S. Qiu, *Chem. Mater*. **2006.** *18.* 6283.

[23] a)S. Yang, N. P. Evmiridis, *Microporous Mater.* **1996**, *6*, 19. b) T. Tomita, K. Nakayama, H. Sakai, *Microporous Mesoporous Mater.* **2004**, *68*, 71.

[24] H. Hatori, Y. Yamada, M. Shiraishi, M. Yoshihara, T. Kimura, *Carbon*, **1996**, *34,* 201.

[25] a) Y. Cui, H. Kita, K. Okamoto, *Chem. Commun.* **2003**. 2154. b) Y. Cui, H. Kita, K.Okamoto, *J. Mater. Chem.* **2004**, *14*, 924.